



Universiteit
Leiden
The Netherlands

Molecular catalytic assemblies for electrodriven water splitting

Joya, K.S.; Valles-Pardo, J.L.; Joya, Y.F.; Eisenmayer, T.J.; Thomas, B.; Buda, F.; Groot, H.J.M. de

Citation

Joya, K. S., Valles-Pardo, J. L., Joya, Y. F., Eisenmayer, T. J., Thomas, B., Buda, F., & Groot, H. J. M. de. (2013). Molecular catalytic assemblies for electrodriven water splitting. *Chempluschem*, 78(1), 35-47. doi:10.1002/cplu.201200161

Version: Publisher's Version

License: [Licensed under Article 25fa Copyright Act/Law \(Amendment Taverne\)](#)

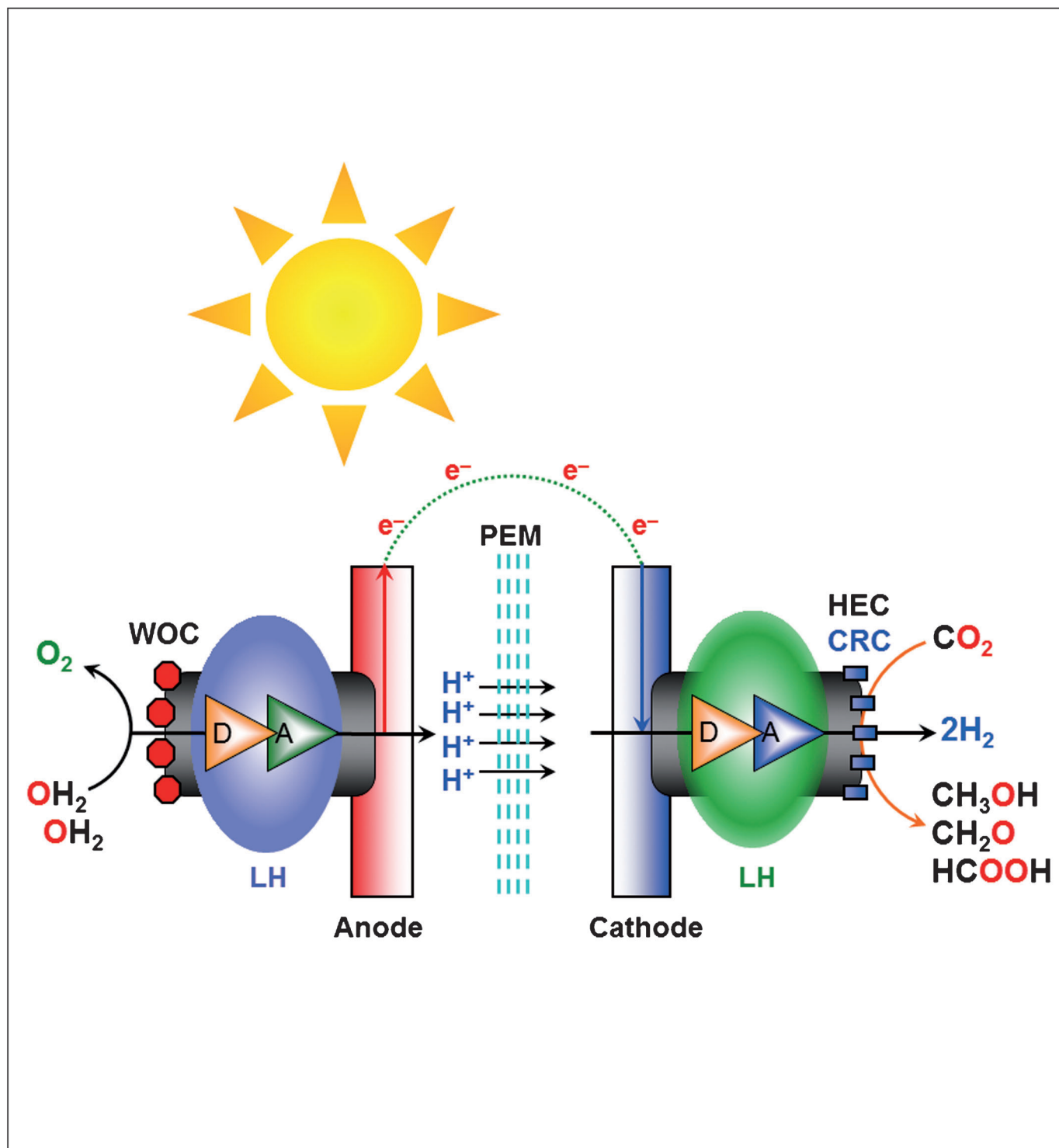
Downloaded from: <https://hdl.handle.net/1887/3422613>

Note: To cite this publication please use the final published version (if applicable).

DOI: 10.1002/cplu.201200161

Molecular Catalytic Assemblies for Electrodriven Water Splitting

Khurram Saleem Joya,^{*,[a, b, c]} Jose L. Vallés-Pardo,^[a] Yasir F. Joya,^[d] Thomas Eisenmayer,^[a] Brijith Thomas,^[a] Francesco Buda,^{*,[a]} and Huub J. M. de Groot^{*,[a]}



Clean energy carriers obtained from renewable, earth-abundant materials and by using the virtually unlimited supply of sunlight have potential to serve as future sustainable power sources. A quest for new materials for oxygen evolution from catalytic water oxidation and carbon dioxide reduction, which aim to build up solar-to-fuel conversion devices that use water as raw material, has been developing during the last two decades. Most of the research in the field of materials science and chemistry has been focused on the development of inorganic materials and molecular complexes for water oxidation, in particular bioinspired catalytic systems. Recently, various molecular water-oxidation complexes with mono- or multinuclear catalytic sites have been tested for solution-phase dioxygen generation. Catalyst immobilization and functionalization

on an electrode surface is required for electrocatalytic or photoelectrochemical water oxidation devices; however, there are only a few examples in which a molecular catalyst has been placed on a transparent conducting surface in an electro- or photoelectrochemical system. Herein, a brief overview of surface-immobilized molecular assemblies for electrochemical water oxidation is presented, and an analysis of recent progress in catalyst design and performance is provided, including systems integration of modules for future stand-alone solar-to-fuel conversion devices. A view on the thermodynamics features of various intermediates and the mechanism of O–O bond formation in single-site complexes and binuclear water oxidation catalysts is also presented.

Introduction

Water can be used as a cheap and renewable source of electrons to make chemical fuels for a sustainable energy supply.^[1,2] The development of a stable, robust, and competent catalytic material for efficient water splitting for the generation of molecular oxygen with simultaneous release of protons is considered a key step in constructing an artificial photosynthetic device.^[3–5] Production of hydrogen or carbon-based fuels by using sunlight and starting from water as the raw material represents a potential solution for carbon dioxide capture as well as environmentally clean and renewable fuel sources.^[5–8] However, designing and constructing a robust and efficient catalytic material for water oxidation to evolve O₂ is considered a challenge, and poses a major obstacle for the implementation and exploitation of electrochemical and photoelectrochemical modular devices (Figure 1).^[9–12]

The chemistry of water oxidation is a complex process and is an energy-intensive reaction involving the removal of four electrons. The natural photosystem II (PS-II) embedded in the thylakoid membrane in plant leaves represents an excellent paradigm for designing an artificial photosynthesis device, since it shows how a self-repairing structural framework can be implemented to couple efficient charge separation with a four-

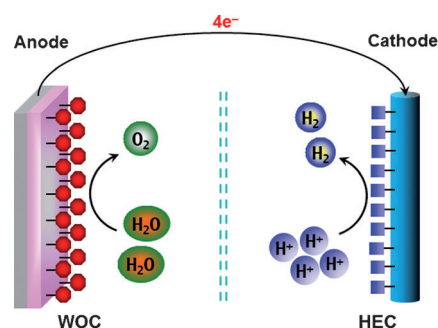


Figure 1. Schematic representation of a photoelectrochemical water oxidation system showing water oxidation catalyst/complex (WOC) at the anode and H₂ evolution catalyst (HEC) at the cathode.

step proton-coupled electron-transfer pathway.^[13,14] Cyclic light-induced activation of P680 chlorophylls leads to the formation of a P680⁺⁺ cation radical by charge separation. The P680⁺⁺ is re-reduced by the oxidation of tyrosine Yz. This prepares the Mn cluster towards water oxidation by extracting electrons (Figure 2).^[15] The recently resolved structures of the Mn_xCaO_y water oxidation complex provide profound insight into the architecture of the catalytic system, OH₂ binding, and arrangements of many water molecules in the vicinity that possibly provide an extensive hydrogen-bonding network facilitating the proton channeling.^[16–18] Various scientific attempts have been made so far to construct a model biomimetic analogue of PS-II, aiming for high catalytic turnover number (TON) and turnover frequency (TOF), with low activation barriers and oxygen onset overpotential and high current densities. However, none of the systems matches the robustness and performance of the PS-II for generating oxygen and protons with high activity and reaction rate.^[19–24]

A modular catalytic device needs to have the following basic structural units and features: 1) an antennae system for efficient light harvesting; 2) long-lived charge-separating components; 3) a robust four-electron-transfer water oxidation catalyst; 4) self-healing, self-generation, and self-assembling of the

[a] Dr. K. S. Joya, J. L. Vallés-Pardo, T. Eisenmayer, B. Thomas, Dr. F. Buda, Prof. H. J. M. de Groot
Leiden Institute of Chemistry, Leiden University
P.O. Box 9502, 2300 RA Leiden (The Netherlands)
Fax: (+31) 71-5274603
E-mail: khurrams@chem.leidenuniv.nl
f.buda@chem.leidenuniv.nl
ssnmr@chem.leidenuniv.nl

[b] Dr. K. S. Joya
Max Planck Institute for Chemical Energy Conversion
Stiftstrasse 34–36, 45470 Mülheim an der Ruhr (Germany)

[c] Dr. K. S. Joya
Department of Chemistry, University of Engineering and Technology
GT Road, Lahore, Punjab 54890 (Pakistan)

[d] Dr. Y. F. Joya
Corrosion and Protection Centre, The Mill
School of Materials, The University of Manchester
Manchester M13 9PL (UK)

oxygen evolution complex; and 5) a consecutive four-step proton-coupled electron-transfer pathway for the device as a whole to avoid high-energy intermediates during O–O bond formation leading towards dioxygen generation.^[25,26] Good scientific progress was obtained in the field of light-harvesting units and charge-separation systems during the last 15 years,^[27–29] and an important hurdle in artificial photosynthesis research is the construction of a synthetic water-splitting

Khurram Saleem Joya is a lecturer at the Chemistry Department, University of Engineering and Technology, Lahore (Pakistan). After his PhD and postdoctoral research at Leiden University (Netherlands), he joined the Max Planck Institute for Chemical Energy Conversion (Mülheim, Germany), in the ESF-framework SolarFuel Tandem, to develop solar fuel devices and water-splitting catalysis. His research interests deal with clean and renewable energy, artificial photosynthesis/leaf, biomimetic approaches towards O₂ and H₂ evolution from catalytic water splitting, CO₂ capture/reduction, electro- and photoelectrochemical catalysis systems, and solar fuel assemblies.



Huib de Groot holds a PhD in physics from Leiden University. After a period at MIT he joined the chemistry faculty in Leiden. He works on photosynthesis, biomimetic catalysts, and multiscale modeling for the design of modular nanodevices for solar fuel. He coordinated the ESF science policy brief on solar fuel, is on the board of the Euro-SolarFuel Eurocores program, and coordinates one of its collaborative research programs. Dr. de Groot serves as the scientific director of the Dutch BioSolar Cells public-private partnership, and contributes to its research, valorization, and innovation projects.



Francesco Buda is an assistant professor at the Leiden Institute of Chemistry. After his PhD in condensed matter physics at the International School for Advanced Studies (Trieste, Italy), he worked at the Ohio State University, IBM Zurich Research Laboratories, Scuola Normale Superiore in Pisa, and the Free University in Amsterdam. His main expertise is in ab initio molecular dynamics simulations and density functional theory calculations, which he is currently applying to investigate molecular mechanisms and chemical reactions relevant to natural and artificial photosynthesis.

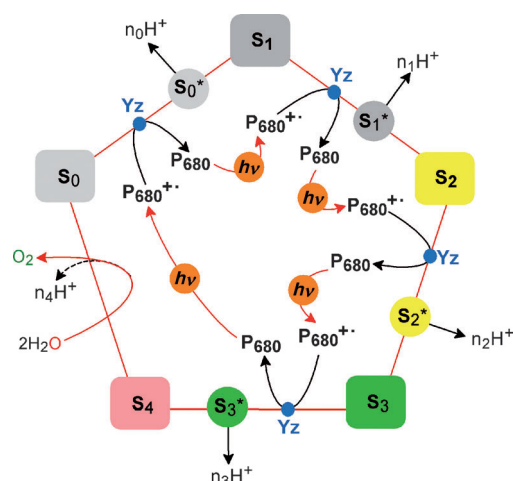


Figure 2. Extended Kok cycle of light-induced water oxidation driven by P680⁺⁺ cation radical with tyrosine (Yz) acting as intermediate. The S_{1–4} transient states are indicated by asterisks. (The exact pathway of proton release is not known yet.)

catalyst capable of performing the light-driven multielectron oxidation reaction for hundreds of thousands of cycles and with swift O–O bond formation to facilitate dioxygen release at a high rate.^[22,23] Like the natural system, a modular photoelectrochemical device should also possess an excellent mechanism for proton management, to shuttle protons at the reduction site to make hydrogen or carbon-based liquid fuels.^[18]

During the last few years, there has been a flurry of scientific activity towards expanding the structural understanding of the PS-II, its water oxidation mechanism, and the O–O bond formation pathway, as well as establishing a synthetic catalyst for proficient water oxidation.^[14–18] There is a whole variety of chemical species, inorganic oxides and composite materials, precious metal molecular complexes and transition-metal organometallics, and multinuclear as well as single-site oxygen-evolving catalysts, which have been tested for water oxidation, heterogeneously and in the solution phase with a chemical catalyst activator.^[30–33] In this Minireview, we present a collection of knowledge and information obtained during the last decade, and the most recent developments in the field of artificial photosynthesis, pursuing towards water oxidation and oxygen generation catalysis. We focus on the progress in surface-anchored and electrode-modified electrochemical water oxidation systems derived from molecular assemblies. Single-site, binuclear, and multicenter complexes studied under different conditions are discussed. An innovative perspective on the smart matrix architecture of electrochemical and photoelectrochemical device systems is presented as well.

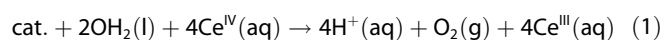
Homogeneous and Heterogeneous Water Oxidation Catalysis

A molecular species can be investigated for water-splitting catalysis either by suspension in homogeneous solution or on the surfaces of nanoparticles, inorganic oxides, and conducting anodic materials.^[13,21] The initial testing stage for a molecular

oxygen-evolving complex generally is to induce the catalysis by using a chemical oxidant or catalyst activator. The most commonly used chemical oxidant for water oxidation by molecular complexes in aqueous solution is cerium ammonium nitrate $(\text{NH}_4)_2[\text{Ce}(\text{NO}_3)_6]$ (CAN), whereas some reports describe the use of NaIO_4 as primary oxidant.^[34] Oxides of transition metals, such as RuO_2 , IrO_2 , CoO_2 , and MnO_2 , and other mixed inorganic materials have been studied extensively for water oxidation in heterogeneous systems and in electrochemical assemblies; however, these materials are required usually in bulk quantities for application in catalytic systems.^[35,36] Recently the integrity of molecular complexes in highly oxidative conditions during water oxidation has been questioned and some catalysts have been turned down as molecular species for oxygen generation in homogeneous catalysis with chemical oxidants.^[37,38] The catalytic system of the discussion herein focuses on the molecular metal complexes and organometallics assemblies that have been studied for water-splitting reactions on surfaces, either electrochemically or photoelectrochemically.

Water splitting in the solution phase with chemical oxidant(s) as catalyst activator

For the investigation of dioxygen formation from catalytic water oxidation by molecular complexes with CAN as catalyst activator, catalytic species are suspended in the homogeneous phase, in aqueous acidic solutions, and Ce^{IV} is added externally in excess to activate the metal complex [Eq. (1)]:^[39,40]



Aqueous perchloric acid (HClO_4) is a widely employed medium for Ce^{IV} to study water oxidation by molecular complexes, since the bulky perchlorate (ClO_4^-) counterions have little tendency to ligate and form complexes with the metal center.^[21–23] CAN, with its tetravalent cerium, is a monomeric species in aqueous solution that is thought to act as a single-electron oxidant.^[37,41,42] However, a combined study by extended X-ray absorption fine structure spectroscopy and density functional theory (DFT) calculations has revealed that Ce^{IV} in CAN makes a unique oxo- and/or hydroxo-bridging binuclear complex in aqueous solution, and recent data obtained for ruthenium-derived catalysts provide evidence that part of the oxygen that is generated originates from the nitrate ions (NO_3^-) of the CAN rather than from H_2O .^[13,41–43] Another important issue is the concentration of the chemical oxidant, which is considerably higher than for the molecular complex, and the presence of high concentrations of oxidant probably promotes decomposition or decay of the catalyst.

Surface electrochemical/electrodriven water oxidation systems

Although catalyst functionalization on a conducting surface may be considered an important step for constructing electro- or photoelectrochemical systems for catalytic water electrolysis, the number of reports in which a molecular catalyst has

been tested on a conducting surface in an electro- or photoelectrochemical system is surprisingly limited.^[3,23] A molecular water-oxidation complex can be simply adsorbed on an electrode exterior, that is, physisorption of catalyst molecules on solid surfaces through the van der Waals forces, or covalently attached to the surface by modification of the catalytic system for interfacing, depending on the nature of anodic material. For conducting oxide surfaces, carboxylic $[-\text{O}-(\text{C}=\text{O})-]$, phosphonate $[-(\text{O})_2-(\text{P}=\text{O})-]$, or silyl $[-(\text{O}_3)-\text{Si}-]$ functionalities have been shown to make a covalent linkage with TiO_2 , SnO_2 , or indium tin oxide (ITO).^[44] Thiol units can also be introduced to establish a sulfide/thio ($-\text{S}-$) linkage with Au, Ag, or CdS surfaces.

In covalently bound surface catalytic assemblies, the electrons, which come from the oxidation of OH_2 , transfer from the molecular catalyst module to the electrode through the linker units by electron tunneling. Therefore, the linkage stability and balancing of the electronic communication or tunneling rate at the interface between the molecular complex and the anodic surface is crucial to obtain an optimal performance of the electrochemical system.^[45a] The phosphonate anchoring groups bind more strongly to the oxide surface than carboxylic linkers, and the linkages are stable at $\text{pH} \geq 9$. However, the affinity of these anchoring units with oxide surfaces is weakened in the presence of pure organic solvents and aqueous–organic mixtures.^[45b] Silyl anchoring groups, on the other hand, represent excellent linkers for oxide exteriors as they have stronger affinity to make stable Si–O linkages. Although the chemically inert silyl, Si–O, bonds contribute to good strength and stability, water oxidation complexes with silyl modification have not yet been studied for surface binding.^[45b]

Photoelectrochemical water oxidation and oxygen evolution

In electrodriven water electrolysis systems, the potential demand for the oxygen evolution reaction can be reduced by employing a photosensitizing material between the catalyst molecule and the electrode. Ideally, a photosensitized electrochemical water oxidation assembly requires little or no overpotential in the presence of light to drive the catalysis process. The most frequently used photosensitizing molecule is $[\text{Ru}(\text{bpy})_3]^{2+}$ ($\text{bpy} = 2,2'$ -bipyridine), although porphyrin-based materials have also been employed.^[46] $[\text{Ru}(\text{bpy})_3]^{2+}$ has received much attention because of its distinctive optical and photophysical properties. It absorbs UV light as well as light in the visible region and has a relatively long-lived excited-state lifetime. It shows reversible redox processes, and displays good stability in the ground and excited states.^[47,48] An aqueous solution of the dye absorbs at (452 ± 3) nm with an extinction coefficient of $11\,500 \text{ M}^{-1} \text{ cm}^{-1}$. The excited state has a relatively long lifetime of 890 ns in acetonitrile and 650 ns in water.^[49] A novel and promising class of sensitizers are multinuclear dendrimers containing Ru^{II} and Os^{II} centers. These materials are proposed to be good photosensitizers for light-induced water-splitting reactions because of favorable redox behavior and photophysical properties.^[25,50]

Molecular Catalysts for Oxygen Evolution

Although the natural PS-II machinery has inspired many researchers to construct a biomimetic catalytic structure for efficient water oxidation, the chemical design of an ideal system operating with four consecutive proton-coupled electron-transfer steps to generate oxygen and protons for hundreds of thousands of cycles at high rate is a formidable challenge.^[51] The quest for a molecular catalytic system that can generate dioxygen from water oxidation started in the early 1970s with the introduction of a di- μ -oxo-bridged dimanganese (Mn^{III} – Mn^{IV}) 2,2'-bipyridine complex by Calvin.^[52] Following this work and using essentially the same ligand architecture, the next decade of research focused on synthetic model complexes with binuclear ruthenium and manganese motifs.^[9,13] Only recently, some molecular catalysts that perform the water oxidation reaction in solution with a mononuclear catalytic site and with other metals such as iridium and iron were reported.^[3,34] Very recently, a homogeneous oxygen-evolving catalyst with a single ruthenium site having a 6,6'-dicarboxylic acid-2,2'-bipyridine (dcabpy) ligand with two isoquinoline (isq) units instead of the previously reported 4-methyl pyridine motif was reported by the groups of Llobet and Sun (Figure 3). In acidic

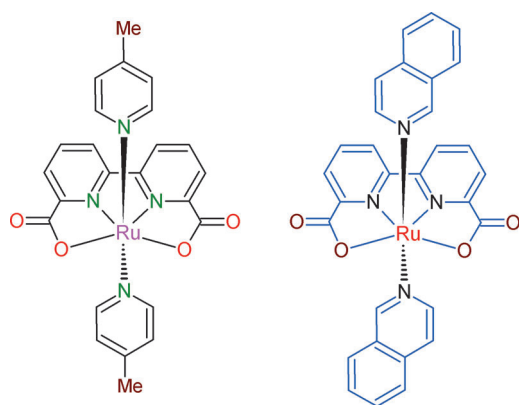


Figure 3. Structure of the 6,6'-dicarboxylic acid-2,2'-bipyridine (dcabpy) ligand with two 4-methylpyridine units and isoquinoline (isq) motif.

solution containing an excess of Ce^{IV} , the catalyst $[\text{Ru}(\text{dcabpy})_2(\text{isq})_2]$ shows an unprecedented oxygen generation rate of more than 300 s^{-1} under homogeneous conditions.^[53] Moreover, the complex produced a TON in excess of 8000, thus indicating very good stability of the catalyst. As rate and robustness are essential design parameters, this system has potential to be employed in light-driven devices for making solar fuels, provided it can be properly immobilized and structurally embedded.

Electrocatalytic Molecular Assemblies for Water Oxidation

To make a solar-to-fuel conversion system, stable and efficient molecular water-oxidation modules are required. For this purpose catalysts can be immobilized and interfaced to a conduct-

ing electrode surface and tested for electrodriven catalysis.^[54] In electrochemical assemblies, the potential needed to drive water splitting and the current densities at which oxygen gas is generated at a high rate are very important parameters that mark the stability and efficiency of the catalytic system.^[3,23] There are very few examples of electrocatalytic water splitting with molecular complexes anchored to an inert electrode exterior.^[21] The standard thermodynamic electrochemical potential required to split water into H_2 and O_2 molecules is $E = 1.23 \text{ V}$ (versus normal hydrogen electrode, NHE) at pH 0, and 0.82 V (vs. NHE) at pH 7, but the immobilized catalyst systems require some additional energy to drive the conversion, usually 0.5 – 0.7 V overpotential above the thermodynamic limit of 1.23 V , under similar conditions of pH and temperature. This is generally owing to the involvement of rate-restraining high-energy intermediates and ohmic resistance in the system.^[13,31] A good electrochemical water-splitting system, in combination with a stable molecular catalyst, should be designed in such a way to cut down the extra potential to a level at which the onset of water oxidation catalysis occurs at 1.23 V and the system operates without significant ohmic losses in an almost linear nonequilibrium steady-state thermodynamic conversion process.^[3]

Ruthenium-based water oxidation assemblies

Among the few ruthenium-derived mono- and binuclear molecular water-oxidation complexes that have been investigated for electrodriven oxygen evolution is the ruthenium trimer complex $[(\text{NH}_3)_5\text{Ru}-\text{O}-\text{Ru}(\text{NH}_3)_4-\text{O}-\text{Ru}(\text{NH}_3)_5]^{6+}$, which was adsorbed on a platinum black electrode and tested for electrocatalytic water oxidation. At 1.3 V (vs. Ag/AgCl) in 0.1 M aqueous acids, a TOF of 1500 h^{-1} ($\approx 0.42 \text{ s}^{-1}$) was reported, which implies that the onset of oxygen evolution occurs very close to the thermodynamic minimum of 1.23 V (pH 0, vs. NHE) for this trinuclear and strongly protic compound.^[55] This is of interest, in view of the latest X-ray results on PS-II, which reveal an extensive protic surrounding of the natural multinuclear Mn_4CaO_5 cluster that is known to operate at 1.23 V , that is, without a significant overpotential loss from the inequality of ΔG steps. In a different promising approach, a bis(ruthenium-hydroxo) complex with a 1,8-bis(2,2':6',2''-terpyridyl)anthracene (btpyan) bridging motif was adsorbed on an ITO electrode and tested for anodic water oxidation (Figure 4a). At $+1.7 \text{ V}$ (vs. Ag/AgCl) in a pH 4 solution, this electrochemical system generates more than 33 500 turnovers in 40 hours of electrolysis with $J = 0.12 \text{ mA cm}^{-2}$.^[56,57]

A homogeneously studied Hbpp-Ru-terpy dimer (bpp = bis(2-pyridyl)-3,5-pyrazolate, terpy = terpyridyl) was modified with an electropolymerizable alkyl pyrrole linker, 4'-(para-pyrrolylmethylphenyl)-terpy, for electrochemical water oxidation. The system produced a TON in excess of 120 at 1.17 V (vs. Ag/AgCl) in a 0.1 M aqueous triflic acid medium.^[58] To make a linker-modified electrocatalytic system, a 2,6-bis(1-methylbenzimidazol-2-yl)-pyridine (Mebimpy) ligand was introduced, instead of the conventional terpy motif, to form the 4,4'-dialkyl phosphonate 2,2'-bpy (4,4'-($\text{H}_2\text{O}_3\text{PCH}_2$)₂-bpy). Anodic water oxi-

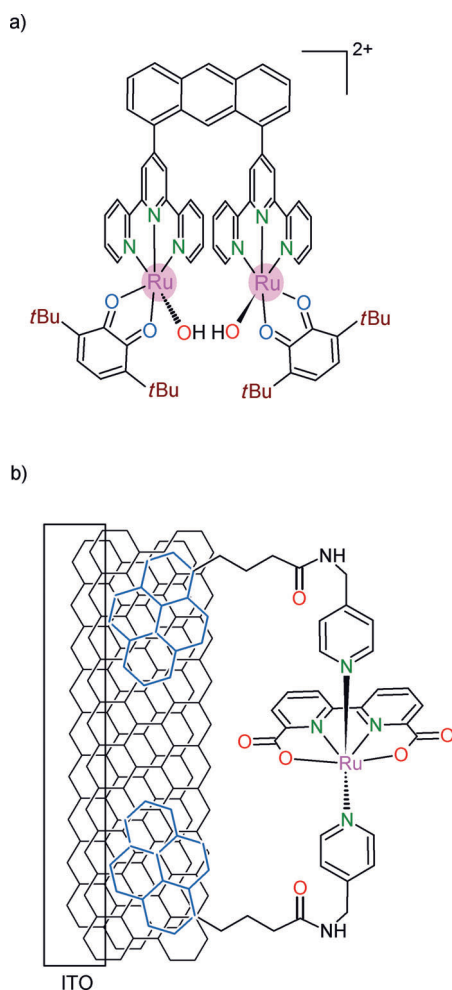


Figure 4. Electrodriven water oxidation assemblies derived from (a) a novel bridging mode 1,8-bis(2,2':6',2''-terpyridyl)anthracene (btptyan) bearing bis(ruthenium-hydroxo) molecular complex; (b) a monomeric bis(pyrene) linkers-modified [Ru(dcabpy)(pic)₂] (dcabpy = 6,6'-dicarboxylic acid-2,2'-bipyridine, pic = 4-picoline) complex immobilized on a MWCNT/ITO assembly, for surface electrochemical water oxidation.

dation was realized at >1.85 V (vs. NHE) in pH 5 buffer, albeit at a very slow turnover rate of 0.004 s^{-1} with a low oxygen yield of $6.5\text{ }\mu\text{mol}$ during approximately 8 hours of controlled potential electrolysis.^[45a] A Ru-tris-bpy type redox mediator with dialkyl phosphonate units was incorporated with [Ru^{II}-(bpm)(terpy)-(OH)₂] (bpm = 2,2'-bipyrimidine) and [Ru^{II}-(bpm)-(Mebimpy)-(OH)₂] complexes for electrodriven water oxidation. At about 1.80 V (vs. NHE) in an acidic medium, 28 000 turnovers were obtained at a rate of 0.6 s^{-1} and with a low current density $J < 50\text{ }\mu\text{A cm}^{-2}$.^[59] In another study, a [Ru(dcabpy)(pic)₂] mononuclear complex (pic = 4-picoline), modified with pyrene-type linkers on each picoline unit, was immobilized on a multi-walled carbon nanotube (MWCNT)/ITO assembly for electrocatalytic water oxidation (Figure 4b).^[60] The system was very stable and efficient, operated at 1.4 V (vs. NHE) in a neutral solution, and produced more than 11 000 TON for molecular oxygen from water at a current density of about 0.22 mA cm^{-2} , sustained for many hours.

Anodic water oxidation by iridium complexes

The anodic deposition of 0.1 M KNO₃ (pH 6) containing pentamethylcyclopentadienyl (Cp*)-Ir aqua or hydroxo species (Ir tris-aqua complex) generates a thin blue layer of an active catalytic material for electrochemical water oxidation.^[61] The blue layer deposit operates with an oxygen evolution current density of approximately 1.4 mA cm^{-2} at 1.4 V (vs. NHE) in a pH 6 electrolyte solution. Although other iridium catalytic precursors under anodic electrocatalytic conditions form a heterogeneous species on the electrode that catalyzes water oxidation, in situ electrochemical quartz crystal nanobalance measurements revealed that a triflate-bonded Cp*-Ir complex with a 2-(2'-pyridyl)-2-propanolate ligand does not give rise to deposition during electrodriven water oxidation, which is taken as strong evidence that the molecular homogeneity of the complex stays intact during the catalysis process.^[38] Recently, we have described efficient electrodriven mono-iridium catalysts anchored on an ITO surface through COOH and PO₃H₂ linkers, which generate more than 200 000 TON for oxygen generation at a TOF of $>6.7\text{ s}^{-1}$.^[62] This system is sustained for many hours and shows a current density of more than 1.75 mA cm^{-2} at 1.75 V (vs. NHE) in a pH 4 solution (Figure 5). Further steps are in progress to incorporate this system into a light-assisted electrochemical catalysis assembly for water splitting.

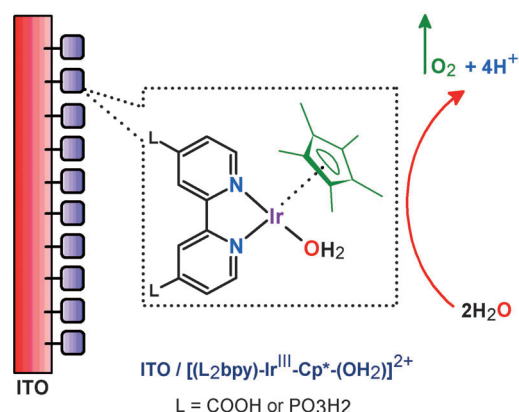


Figure 5. A surface-immobilized electrochemical water oxidation assembly showing Cp*-iridium-derived complexes with L₂bpy ligands for electrodriven oxygen evolution.

A self-assembled Cu-bpy water oxidation electrocatalyst

Iridium and ruthenium are among the precious metals that offer little perspective for large-scale terrestrial applications in water electrolysis systems. However, a copper bipyridine (Cu-bpy)-derived electrocatalyst for anodic water oxidation was reported that shows a very high activity and rapid rate for the oxygen evolution reaction.^[63] The Cu-bpy hydroxo complex [Cu₂(bpy)₂(μ-OH)₂]²⁺ self-assembles in situ from a copper salt and bpy ligand in a pH > 11 solution (Figure 6). The cyclic voltammetry of the complex on glassy carbon (GC) and ITO elec-

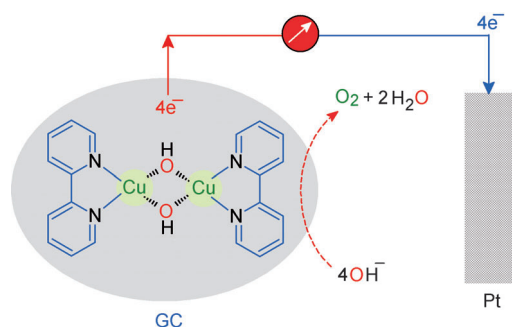


Figure 6. A self-assembled copper-bipyridine dihydroxo $[\text{Cu}_2(\text{bpy})_2(\mu\text{-OH})_2]^{2+}$ water oxidation electrocatalyst.

trodes shows a large irreversible catalytic current wave at pH 11 to 13. Spectroscopic studies and electrochemical experiments reveal that the catalyst is a soluble molecular species and among the best known homogeneous systems for electrochemical water oxidation. In a controlled experiment with a fluorescent probe, the catalyst displays a TOF of approximately 100 s^{-1} . However, the system operates at a high overpotential, 700–900 mV in alkaline medium. This may limit its application for the oxygen evolution reaction in a water electrolysis setup.

Light-Induced Catalytic and Electrochemical Water Oxidation Systems

In addition to the development of catalytic materials for water splitting to make molecular oxygen and hydrogen chemically or electrocatalytically, initial steps were taken to combine a molecular water-oxidation complex with a photochemical charge-separation unit to establish a light-driven electrochemical system.^[20] The grand challenge here is the chemical design of a synergistic combination of a molecular catalyst with a light-harvesting system that drives the photoelectrochemical water oxidation with high efficiency, close to the thermodynamic limit. For a light-induced electrochemical system, four key components are required: 1) a competent and chemically stable water oxidation catalyst; 2) an efficient light-harvesting photosensitizing material with high molar absorptivity; 3) a molecular donor–acceptor pair or redox ladder for effective charge separation; and 4) a conducting electrode surface or a semiconducting material.^[36,64] In addition, the water-splitting catalyst should be a light-stable metal complex, chemically and thermodynamically compatible with the photosensitizing material, and accessible to water and protons.^[64,65] Below, we give an overview of recent studies regarding photoelectrochemical water oxidation assemblies.

Ruthenium complexes for photoelectrochemical catalysis of water

The mono-site bpy ruthenium complexes with terpy and Me-bimpy ligands, with incorporation of a Ru-tris-bpy type photosensitizer, were studied electrochemically on conducting surfaces. In this configuration the Ru-tris-bpy unit acts as a redox

mediator rather than a photosensitizer. Water oxidation was realized at about 1.80 V (vs. NHE) both with and without the photosensitizer. The effect on the water oxidation overpotential in the presence of the photosensitized unit in the catalyst was negligible.^[59] In another study, a mono-Ru complex $[\text{Ru}(\text{dcabpy})(\text{pic})_2]^+$, with onset of catalysis at approximately 0.98 V (vs. NHE) at pH 7, was suspended in a Nafion matrix on a $[\text{Ru}(\text{bpy})_3]^{2+}$ -sensitized TiO_2 film on ITO (Figure 7). With

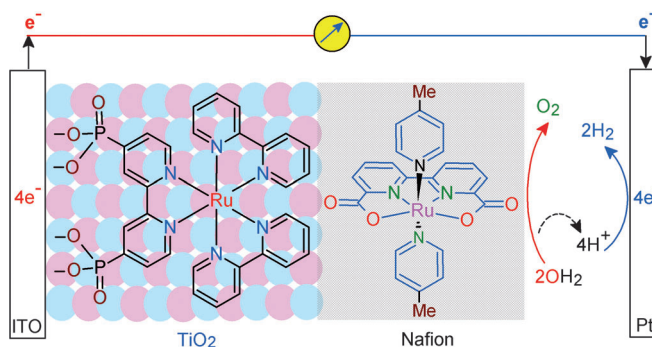


Figure 7. Illustration of a light-driven electrochemical system for complete oxidative conversion of water into H_2 and O_2 . The device comprises a transparent ITO surface sensitized with $\text{di}(\text{PO}_3\text{H}_2)$ -modified Ru-tris-bpy, covered by a mono-Ru complex $[\text{Ru}(\text{dcabpy})(\text{pic})_2]^+$ embedded in a Nafion matrix (dcabpy = 6,6'-dicarboxy-2,2'-bipyridine, pic = 4-picoline).

a small bias potential of -0.325 V (vs. Ag/AgCl), both the photoelectrolysis of water and H_2 formation were detected by gas chromatographic analysis. High acidity of the Nafion was suggested to be the reason for rapid decay of the catalytic performance.^[66]

Cubane-derived systems of Mn and Co complexes

Mn-cubane derived light-driven electrochemical water oxidation

The synthetic tetramanganese complex $[\text{Mn}_4\text{O}_4\text{L}_6]^+$ (L = diphenylphosphinate, $(\text{MeOPh})_2\text{PO}_2^-$) with a $(2\text{Mn}^{\text{III}}-2\text{Mn}^{\text{IV}})$ -cubane core, which represents a biomimetic model for the active site of the photosynthetic water oxidation cluster, was impregnated into a thin Nafion proton-transport membrane on a conducting surface for photoelectrochemical water oxidation studies.^[67,68] With a small bias potential of approximately 1.2 V (vs. NHE) and with visible-light illumination, the photoelectrochemical system generated >1000 catalytic cycles in the aqueous electrolyte at pH 6.5.^[69] Recently, the same Mn-cubane catalyst was impregnated into a Nafion membrane supported on a $[\text{Ru}^{\text{II}}(\text{bpy})_2(\text{COO})_2\text{-bpy}]$ light sensitizer on a TiO_2 film (Figure 8). In this way a photoelectrochemical multilayer device system has been constructed that oxidizes water by using only visible light, without any external bias potential.^[69b] In addition, a detailed study of the catalytic mechanism of the tetramanganese complex $[\text{Mn}_4\text{O}_4\text{L}_6]^+$ in a Nafion membrane was performed by using in situ Mn K-edge X-ray absorption spectroscopy and transmission electron microscopy. The spectroscopic analyses

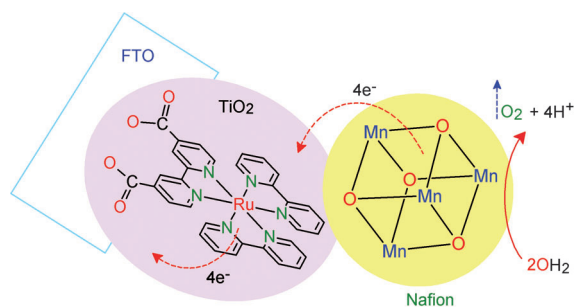


Figure 8. Schematic of a light-driven photoelectrochemical assembly with a tetramanganese ($2\text{Mn}^{\text{III}}-2\text{Mn}^{\text{IV}}$)-cubane catalyst. The Mn-cubane complex is impregnated into a Nafion membrane supported on a $[\text{Ru}^{\text{II}}(\text{bpy})_2(\text{COO})_2^-]$ light sensitizer on TiO_2 film. FTO = fluorine tin oxide.

reveal that there is a dissociation of the Mn-cubane within the Nafion polymer matrix that generates Mn^{II} -type compounds. Subsequent electrochemical oxidation to form $\text{Mn}^{\text{III/IV}}$ oxides possibly leads to water oxidation, instead of water splitting by a molecular homogeneous species.^[70]

Co_4O_4 core cubane complex

Following the work on the Mn-oxo cubane water oxidation electrocatalysis, a Co_4O_4 cubane complex $[\text{Co}_4\text{O}_4(\text{OAc})_4(\text{py})_4]$ (py = pyridine) was reported that can be powered for oxygen evolution, either by a photochemical oxidation source or by electrochemical means.^[71] Similar compounds were reported earlier but never tested for water oxidation.^[72,73] Cyclic voltammetry of the cobalt complex in acetonitrile shows a one-electron reversible redox couple at $E_{1/2} = 0.71$ V (vs. Ag/AgCl), which corresponds to the $\text{Co}^{\text{III}}, \text{Co}^{\text{IV}}$ electronic transitions. A light-driven photochemical cell study was conducted with the Co-cubane catalyst sensitized with $[\text{Ru}(\text{bpy})_3]^{2+}$ in a persulfate ($\text{Na}_2\text{S}_2\text{O}_8$) solution. On light illumination, the catalytic system generates 40 TON in 1 hour of operation at an oxygen generation rate of $0.02 \text{ mol cat}^{-1} \text{ mol s}^{-1}$.^[73] The catalytic activity of the Co_4O_4 cubane complex resembles the action of the Mn analogue, which is ascribed to the presence of a cubic core that is very similar to the natural CaMn_4O_5 water oxidation cluster in PS-II.

Polyoxometalate-Derived Water Oxidation System

Polynuclear Ru-polyoxometalate for electrochemical and catalytic water oxidation

A novel paradigm in water oxidation catalysis was introduced a few years ago with the example of a polyoxometalate (POM) diruthenium-substituted electrocatalyst for oxygen evolution.^[74] A POM is an inorganic structure with two metal sites bridged by oxygen and hydroxo units and is potentially more robust than the organic molecular catalysts, at the same time allowing for chemical engineering for optimal catalytic performance. X-ray diffraction measurements and elemental analysis reveal a diruthenium compound $\text{Na}_{14}[\text{Ru}^{\text{III}}\text{Zn}_2(\text{H}_2\text{O})_2-$

$(\text{ZnW}_9\text{O}_{34})_2]$, and the distance between the two Ru atoms is relatively short, 0.318 nm. This is considered to be an important factor for water oxidation and O–O bond formation. The electrodriven experiments were conducted on a gold surface in aqueous phosphate buffer (pH 8). A catalytic current was observed at 0.55 V that increased with the applied potential up to a maximum of 1.05 V. A Tafel slope of approximately 120 mV was observed, which effectively excludes the formation of Ru oxide during catalysis.^[74] This work was followed by two reports that describe POM-based catalysts with a tetraruthenium core for solution-phase water oxidation.^[75,76] At pH 0.6 in water, 385 μmol of O_2 was generated, which corresponds to a 90% yield based on the added Ce^{IV} oxidant, with a TON = 90.^[74] Recently, the tetraruthenate core POM assembly was integrated with a MWCNT/ITO surface to form a nanostructured oxygen-evolving assembly for electrochemical water oxidation (Figure 9). In a pH 7 solution, TOFs of 36–306 were obtained, depending on the applied potential, and higher than in the

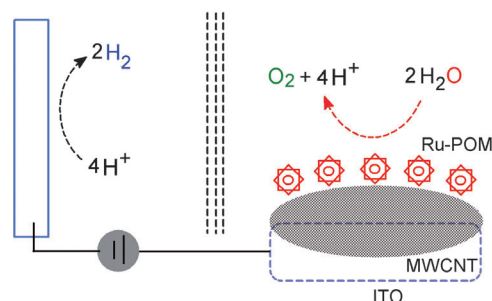


Figure 9. Nanostructured oxygen-evolving material comprises a tetraruthenate core POM integrated with a MWCNT surface on an ITO anode for electrochemical water oxidation.

previous practices. The excellent performance of the system is attributed to the synergistic coupling of the $\text{Ru}_4\text{-POM}$ with the MWCNT on the ITO surface, which provides good electrical plugging of the hybrid material to make the nanoscale structure.^[77]

Cobalt polyoxometalate complex for water splitting

Recently, a POM-derived complex containing four cobalt centers with a Co_4O_4 core, $[\text{Co}_4(\text{H}_2\text{O})_2(\text{PW}_9\text{O}_{34})_2]^{10-}$, was investigated as a homogeneous water oxidation catalyst, and showed a high $\text{TOF} \geq 5$ in pH 8 solution with $[\text{Ru}(\text{bpy})_3]^{2+}$ as oxidant. The catalytic TONs were only 75.^[78] The initial spectroscopic, electrochemical, and inhibition studies indicated that the Co-POM is a stable catalyst and there was no evidence for the formation of hydrated cobalt ions or cobalt hydroxide/oxide. However, combined electrochemical experiments, kinetic studies, UV/Vis analyses, SEM, and energy-dispersive X-ray data provide converging and compelling evidence for the formation of a heterogeneous Co oxide species as the water oxidation catalyst, instead of a homogeneous $[\text{Co}_4(\text{H}_2\text{O})_2(\text{PW}_9\text{O}_{34})_2]^{10-}$ catalytic system for oxygen evolution.^[79]

Thermodynamic Considerations and Computational Tools in Studying Water Oxidation Reactions

Free energy of the intermediates along the water oxidation cycle

The total free-energy change (ΔG) for the complete water-splitting catalytic cycle ($2\text{H}_2\text{O} \leftrightarrow \text{O}_2 + 2\text{H}_2$) is $\Delta G = 4.92$ eV in a pH-independent representation of the reaction coordinate, and is assumed to be distributed over four proton-coupled electron-transfer steps $\text{S}_0 \rightarrow \text{S}_4$.^[80] The electrolysis of water requires always some excess energy in the form of an overpotential, to sustain the conversion and to prevent back reaction of the product.^[80] Based on computational work it has been suggested that the overpotential is related to the different binding energies of the catalytic intermediates that are related to each other by scaling relations.^[81, 82] The total free-energy change for water splitting is fixed at 4.92 eV, so a decrease of one step, below 1.23 eV, implies an increase of one or more other steps, and because the largest step determines the total potential needed to drive the reaction, the variation between steps along the reaction coordinate is a good measure of the efficiency that can be obtained with a catalyst. The goal is thus to make a catalyst with a reaction coordinate that has four equal steps with the same $\Delta G = 1.23$ eV.^[82]

With recent advancements in computational chemistry it is possible to estimate the free-energy differences between the intermediates and the ΔG steps along the reaction coordinate with good accuracy from DFT calculations. To predict computationally the best catalyst for the water oxidation process, three contributions to the ΔG value are taken into account, according to Equation (2):^[83, 84]

$$\Delta G = \Delta H + \Delta \text{ZPE} - T\Delta S \quad (2)$$

in which ΔH is the enthalpy difference between the different intermediates ($\text{S}_0 \rightarrow \text{S}_4$), ΔZPE is the change in zero-point energy, which is derived from the frequencies of the vibrational normal modes calculated with DFT, and $T\Delta S$ is the change in entropy obtained by using standard thermodynamic tables for H_2O and H_2 , assuming that the changes of entropy in the catalyst are negligible compared to the other terms.^[85] This method has been used in several studies to analyze the energetics of the catalytic cycle, both for metallic or metal-oxide surfaces^[82] and for molecular catalysts.^[85]

DFT is a suitable and computationally efficient approach to estimate the different terms in Equation (2). The central quantity in DFT is the electron density, which only depends on three spatial coordinates. This represents a simplification compared to the many-electron wave function, which depends on all electronic coordinates and thus its complexity increases with the size of the system ($3N$).^[86] The DFT approach is a very helpful tool that is complementary to the experimental investigations, since DFT calculations can predict with a reasonable accuracy geometrical structures, many molecular properties, reaction mechanisms, and spectroscopic features.^[87, 88]

O–O bond formation and computational study methods

A crucial step in the water oxidation catalytic cycle is the formation of the oxygen–oxygen bond in the $\text{S}_2 \rightarrow \text{S}_3$ step. To improve the efficiency and rate of this step it is important to know in detail the reaction mechanism and the characteristics and complexity of the intermediate products along the reaction path: if the bond formation occurs as a result of an intramolecular recombination or following an external attack; where the released proton goes; and if a spin crossover takes place. The more information about the path is available, the easier it will be to proceed with rational design for the improvement of the catalytic activity. One approach to study chemical reactions in an explicit solvent environment is *ab initio* molecular dynamics (AIMD), in which the nuclei evolve at finite temperature according to forces evaluated from the electronic structure calculated at the DFT level.^[89] Despite continuous advances in both numerical efficiency and computer technology, AIMD simulations are still limited to processes involving a few hundred atoms and occurring within a few tens of picoseconds at most. The number of chemical reactions that take place spontaneously on such a short timescale, however, is fairly limited; typically, energy barriers of many kcal mol^{-1} need to be overcome. A wide variety of computational approaches have been developed over the years to force or speed up chemical reactions in AIMD and to calculate free energies.

One of the most powerful tools in this direction is metadynamics.^[90] Metadynamics is a coarse-grained dynamics on the free-energy surface (FES) defined by a few collective variables (CVs), such as the distance between two atoms, by using an adaptive bias potential to escape from local minima in the FES. At each metadynamics step the evolution of the CVs is guided by a generalized force, which combines the action of the thermodynamic force that would trap the system in a free-energy minimum and a history-dependent force that disfavors configurations already visited. This history-dependent potential is built as a sum of Gaussian functions centered in the explored values of the CVs. With this method it is possible to explore almost freely the reaction pathway overcoming the activation barrier along the CV chosen, the O–O distance in the specific case of the $\text{S}_2 \rightarrow \text{S}_3$ reaction step. Moreover, it provides an estimate of the free-energy profile for the reaction. Recently, new implementations of this tool have been realized, such as well-tempered metadynamics,^[91] multiple walkers,^[92] bias-exchange metadynamics,^[93] and flux-tempered metadynamics.^[94] These implementations allow better explorations of the reaction pathway and the free-energy landscape.^[95–97]

Metadynamics allows a quick sample of the reaction pathway, but could require an unaffordable computational effort to obtain an accurate free-energy plot. An alternative approach to estimate the free energy is thermodynamic integration using constrained molecular dynamics (CMD).^[98] In this method the CV is fixed and the system is equilibrated for different CV values. The Lagrange multiplier associated with the constraint is related to the thermodynamic force applied to the system for keeping the constraint at the desired value and can be

computed along the CMD simulation. The statistical average of this parameter is used in the thermodynamic integration over the CV space to obtain the free-energy profile of the studied reaction.^[99,100] A comprehensive description is obtained if both metadynamics and CMD methods are used in tandem.^[95] First the reaction pathway is determined by using metadynamics simulations, and then, with the knowledge about the pathway, several CMD simulations are performed at different CV values to compute the free-energy profile.

A practical example of the use of metadynamics simulations is the study of the complex $[\text{Ru}(\text{benzene})(\text{bpy})(\text{O})]^{2+}$ in an explicit water environment.^[95] Figure 10 shows the variation of the relevant geometrical parameters describing the oxygen–oxygen bond formation reaction and the molecular representation of the intermediate product. The distance between the oxygen of the water molecule (Ow1) and the oxyl radical (Ox) is the only one driven by the adaptive biasing potential (red line), whereas all other structural changes occur spontaneously. If Ox–Ow1 is about 1.8 Å, an increase in the distance between the ruthenium atom and the oxyl radical (black line) and an increase in the internal distance between the hydrogen (Hw1) and oxygen (Ow1) atoms of the approaching water molecule (blue line) are observed. At the same time a decrease in the distance between the hydrogen of the reacting water (Hw1) and the oxygen of a second water molecule (Ow2) takes place (green line). Soon after the Ox–Ow1 distance has reached a value of approximately 1.4 Å, which indicates the formation of the O–O bond, one hydrogen atom of the reactant water jumps on the second water molecule, thus forming a hydronium ion OH_3^+ .^[95] In Figure 10 (right), a snapshot of the simulation clearly shows the formation of the Ru–OOH intermediate and of a hydronium ion.

Smart Matrices for Solar-to-Fuel Devices

For a photochemical solar-to-fuel converter, the theoretical maximum for the thermodynamic efficiency is rooted in the

microscopic reversibility of the conversion processes according to the detailed balance limit for an optical absorber connected to a linear nonequilibrium chemical network.^[101] From photosynthetic reaction centers it is known that energetically the best way to make a long-living charge-separated state is to proceed through several intermediate redox steps in a supramolecular assembly of dye molecules, rather than using a single donor–acceptor pair.^[102] The best efficiency is obtained with a sequence of barrierless conversion steps that are energetically downhill to buy storage time by kinetic stabilization, and prevent back transfer that leads to fluorescence decay or other losses.^[13] For light absorption and charge separation, mainly porphyrin-type compounds, chlorophylls and pheophytins, are used. Owing to their intrinsic complexity, the proteins that fold around them affect their shape, energetic properties, and reactivity to provide the chemical preprogramming of these compounds for the desired functions of barrierless excitation transfer and charge separation.^[103]

For efficient catalysis by metal centers, kinetic stabilization is also essential, on a much longer timescale of 10^{-4} to 10^{-3} s, in which the self-organization in the catalyst environment is driven by the extraction of electrons across a tunneling barrier. This timescale is 4–5 orders of magnitude longer than the fluorescence lifetime of approximately 10^{-9} s of the absorber, which translates into an electron-tunneling distance of approximately 2 nm.^[104] For stand-alone solar-to-fuel conversion, modules for light harvesting, charge separation, and catalysis will have to be integrated. Time scales, length scales, and energy scales will have to be optimized and connections will have to be adjusted to avoid energy losses.^[102] Initial modular designs for integrated devices that split water and generate hydrogen with light by using supramolecular catalytic modules coupled to dyes have been presented, but the efficiency is low, which results from an unfavorable balance between forward transfer of electrons and back conversion of reaction products followed by recombination of electrons and holes (Figure 8).^[36] For the chemical design of biomimetic charge-separation modules, the

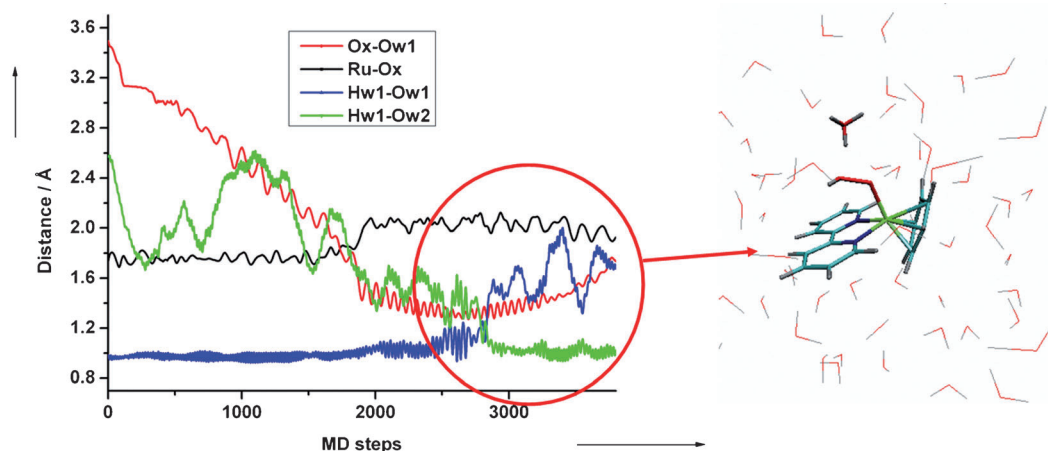


Figure 10. Left: Relevant geometrical parameters along the metadynamics simulation of the solvated $[\text{Ru}(\text{benzene})(\text{bpy})(\text{O})]^{2+}$ complex, in which the Ox–Ow1 distance is the collective variable; see text for a description of the other parameters. Right: Hydroperoxo intermediate in a solvated environment. The hydronium ion formed in the simulation is also highlighted. This snapshot is taken after 1.7 ps of simulation.

chlorosome-based light-harvesting systems, which are self-protected against degradation, provide a good starting point.^[105] Mimics of the natural chlorins can be programmed for self-assembly and have been used to construct artificial photosynthetic materials and a charge-separation unit.

For the design of chemically preprogrammed suprastructures, porphyrin-type systems may be replaced by more robust naphthalene diimide (NDI) and perylene diimide dyes, to perform barrierless light harvesting, charge separation, and catalysis, similar to the natural systems. Diverse kinds of core-substituted NDIs are available with various HOMO–LUMO values and it is possible to combine different NDIs for better energy conversion over the entire solar spectrum (Figure 11).^[106–108] Tuning

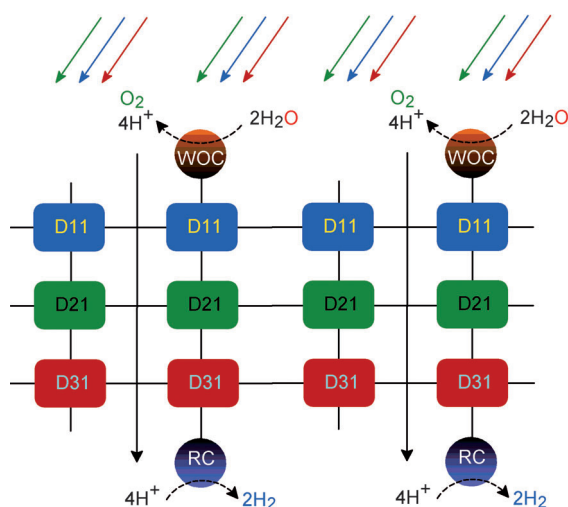


Figure 11. A catalyst integrated into a modular dye array system for light-powered water oxidation and proton reduction. WOC = water oxidation catalyst, RC = reduction catalyst. D11, D21, and D31 are dye units for blue, green, and red light harvesting from solar radiation.

of the energy levels is necessary for application in a tandem cell architecture, for which photons from two spectral regions $\lambda \leq \lambda_1$ and $\lambda_1 < \lambda \leq \lambda_2$ are used in series to provide the additional bias voltage required to reduce the recombination rate for the overall water-splitting reaction.^[107,108] It was estimated that for a realistic energy loss of 0.8 eV per photon, optimal conversion is expected for $\lambda_1 = 720$ nm and $\lambda_2 = 1120$ nm.^[107] Alkyl linkers can be substituted at the nitrogen of the diimide to moderate the transfer of the electrons to the electrode. Linker units can be a carboxylic acid, a phosphate unit, or a hydroxyl group.^[109,110] The planar aromatic nature of NDI helps to stack these molecules in a three-dimensional way to form a supra-molecular assembly.^[111,112] To make sure that electrons flow from higher potential to lower potential across the interfaces with the electrode and the catalyst module, HOMO–LUMO values can be determined by cyclic voltammetry and absorption spectroscopy.^[107,112]

For the implementation of a tandem device, charge-separator and catalyst modules need to be combined. Two types of catalysts are required, for the oxidation of water and for the re-

duction of protons. A proper matching of the time scales, length scales, and energy scales between the catalyst module and the charge-separation module is necessary to promote the forward catalysis reaction and to prevent the recombination of electrons with holes.^[64] An electrode is required to transfer electrons from the oxidation side to the photocathode and the reduction catalyst. A major challenge is in the design of barrierless molecular gates for unidirectional electron flow, to prevent the recombination and decay of charge-separated states in these types of devices. In line with the natural paradigms found in photosynthesis, this can be achieved by switching the molecular overlap in time to reduce the tunneling probability, or by using the characteristics of a semiconductor charge-separation device in combination with a molecular catalyst.

Summary

Establishing a stable and efficient light-induced electrochemical molecular water-oxidation assembly is a key task towards the construction of a surface-immobilized bioinspired system. The capability to make primary energy carriers from water and CO₂ by using abundant sunlight would also stimulate the technological development of carbon capture and conversion systems. To search for and design a competent oxygen-evolving catalyst, significant steps have been made in recent years in the field of water-splitting science and technology. Thermodynamically, water oxidation is an energy-demanding process, but catalyst design biomimicking the Mn₄CaO₅ cluster in the photosynthetic system could make it possible to split water with ease, through small activation barriers and at moderate overpotential. Herein, we give an account of the recent progress made in the design and implementation of molecular catalysts. After briefly covering the homogeneously conducted studies the main focus is on the electrodriven and photoelectrochemical systems for oxidation of water by surfaces functionalized with metal complexes. Different examples are presented of mono-site and multinuclear molecular complexes, with various models for anchoring a molecular complex or array on a conducting surface for electro- or photoelectrochemically powered systems, which have potential to be utilized in future solar-fuel devices. Finally, examples of in situ formation of molecular catalytic assemblies are described that perform well for dioxygen generation, while operating with good current densities and moderate overpotential in electrochemical experiments.

Outlook

The road towards establishing a model photoelectrochemically triggered molecular catalytic system for efficient water oxidation to make clean solar-energy carriers for a greener future is slowly brightening up. However, there is still a long distance to be traveled while going through rational thinking, more scientific input, and experimental demonstrations regarding a practical device for artificial photosynthesis, the artificial leaf. The field of water splitting and catalysis for oxygen evolution is growing more than ever before, and the next step is to com-

bine various components of a synthetic device for efficient and complete conversion of water, sunlight, or carbon dioxide into oxygen, hydrogen, or low-carbon fuels as a chemical medium for renewable energy storage.

Acknowledgements

K.S.J. acknowledges funding from the Higher Education Commission (HEC), Government of Pakistan. The work was also supported in part by the BioSolar Cells program (project numbers C1.6 and C1.9) of the Ministry of Economy, Agriculture, and Innovation of The Netherlands. The use of supercomputer facilities was sponsored by The Netherlands National Computing Facilities Foundation (NCF), with financial support from the Netherlands Organization for Scientific Research (NWO).

Keywords: electron transfer • oxidation catalysis • oxygen evolution • renewable resources • water splitting

- [1] N. S. Lewis, *Nature* **2001**, 414, 589–590.
- [2] T. J. Meyer, *Nature* **2008**, 451, 778–779.
- [3] K. S. Joya, H. J. M. de Groot, *Int. J. Hydrogen Energy* **2012**, 37, 8787–8799.
- [4] T. N. Verziroglu, F. Barbir, *Int. J. Hydrogen Energy* **1992**, 17, 391–404.
- [5] J. E. Funk, *Int. J. Hydrogen Energy* **2001**, 26, 185–190.
- [6] L. Schlapbach, *Nature* **2009**, 460, 809–811.
- [7] E. E. Barton, D. M. Rampulla, A. B. Bocarsly, *J. Am. Chem. Soc.* **2008**, 130, 6342–6344.
- [8] M. M. Najafpour, T. Ehrenberg, M. Wiechen, P. Kurz, *Angew. Chem.* **2010**, 122, 2281–2285; *Angew. Chem. Int. Ed.* **2010**, 49, 2233–2237.
- [9] M. Yagi, M. Kaneko, *Chem. Rev.* **2001**, 101, 21–35.
- [10] J. K. Hurst, *Coord. Chem. Rev.* **2005**, 249, 313–328.
- [11] J. P. McEvoy, G. W. Brudvig, *Chem. Rev.* **2006**, 106, 4455–4483.
- [12] X. Sala, I. Romero, M. Rodríguez, L. Escriche, A. Llobet, *Angew. Chem.* **2009**, 121, 2882–2893; *Angew. Chem. Int. Ed.* **2009**, 48, 2842–2852.
- [13] H. Dau, C. Limberg, T. Reier, M. Risch, S. Roggan, P. Strasser, *ChemCatChem* **2010**, 2, 724–761.
- [14] M. H. V. Huynh, T. J. Meyer, *Chem. Rev.* **2007**, 107, 5004–5064.
- [15] G. Renger, *Biochim. Biophys. Acta* **2012**, 1817, 1164–1176.
- [16] K. N. Ferreira, T. M. Iverson, K. Maghlaoui, J. Barber, S. Iwata, *Science* **2004**, 303, 1831–1838.
- [17] B. Loll, J. Kern, W. Saenger, A. Zouni, J. Biesiadka, *Nature* **2005**, 438, 1040–1044.
- [18] Y. Umena, K. Kawakami, J.-R. Shen, N. Kamiya, *Nature* **2011**, 473, 55–60.
- [19] C. W. Cady, R. H. Crabtree, G. W. Brudvig, *Coord. Chem. Rev.* **2008**, 252, 444–455.
- [20] A. Magnuson, M. Anderlund, O. Johansson, P. Lindblad, R. Lomoth, T. Polivka, S. Ott, K. Stensjö, S. Styring, V. Sundström, L. Hammarström, *Acc. Chem. Res.* **2009**, 42, 1899–1909.
- [21] H. Yamazaki, A. Shouji, M. Kajita, M. Yagi, *Coord. Chem. Rev.* **2010**, 254, 2483–2491.
- [22] L. Duan, L. Tong, Y. Xua, L. Sun, *Energy Environ. Sci.* **2011**, 4, 3296–3313.
- [23] I. Romero, M. Rodríguez, C. Sens, J. Mola, M. R. Kollipara, L. Francàs, E. Mas-Marza, L. Escriche, A. Llobet, *Inorg. Chem.* **2008**, 47, 1824–1834.
- [24] M. Yagi, A. Syouji, S. Yamada, M. Komi, H. Yamazaki, S. Tajima, *Photochem. Photobiol. Sci.* **2009**, 8, 139–147.
- [25] F. Puntoriero, A. Sartorel, M. Orlandi, G. L. Ganga, S. Serroni, M. Bonchio, F. Scandola, S. Campagna, *Coord. Chem. Rev.* **2011**, 255, 2594–2601.
- [26] V. Balzani, A. Credi, M. Venturi, *ChemSusChem* **2008**, 1, 26–58.
- [27] M. Wasielewski, *Acc. Chem. Res.* **2009**, 42, 1910–1921.
- [28] B. Albinsson, J. Mårtensson, *J. Photochem. Photobiol. C* **2008**, 9, 138–155.
- [29] A. C. Benniston, A. Harriman, *Mater. Today* **2008**, 11, 26–34.
- [30] J. T. Muckerman, D. E. Polyansky, T. Wada, K. Tanaka, E. Fujita, *Inorg. Chem.* **2008**, 47, 1787–1802.
- [31] Á. Valdés, Z.-W. Qu, G.-J. Kroes, J. Rossmeisl, J. K. Nørskov, *J. Phys. Chem. C* **2008**, 112, 9872–9879.
- [32] L. Hammarström, S. Styring, *Philos. Trans. R. Soc. B* **2008**, 363, 1283–1291.
- [33] R. Brimblecombe, C. Dismukes, G. F. Swiegers, L. Spiccia, *Dalton Trans.* **2009**, 9374–9384.
- [34] X. Liu, F. Wang, *Coord. Chem. Rev.* **2012**, 256, 1115–1136.
- [35] R. Subbaraman, D. Tripkovic, K.-C. Chang, D. Strmcnik, A. P. Paulikas, P. Hirunsit, M. Chan, J. Greeley, V. Stamenkovic, N. M. Markovic, *Nat. Mater.* **2012**, 11, 550–557.
- [36] W. J. Youngblood, S.-H. A. Lee, K. Maeda, T. E. Mallouk, *Acc. Chem. Res.* **2009**, 42, 1966–1973.
- [37] D. B. Grotjahn, D. B. Brown, J. K. Martin, D. C. Marelus, M.-C. Abadjian, H. N. Tran, G. Kalyuzhny, K. S. Vecchio, Z. G. Specht, S. A. Cortes-Llamas, V. Miranda-Soto, C. van Niekerk, C. E. Moore, A. L. Rheingold, *J. Am. Chem. Soc.* **2011**, 133, 19024–19027.
- [38] N. D. Schley, J. D. Blakemore, N. K. Subbaiyan, C. D. Incavito, F. D'Souza, R. H. Crabtree, G. W. Brudvig, *J. Am. Chem. Soc.* **2011**, 133, 10473–10481.
- [39] N. D. McDaniel, F. J. Coughlin, L. L. Tinker, S. Bernhard, *J. Am. Chem. Soc.* **2008**, 130, 210–217.
- [40] D. J. Wasylenko, C. Ganesamoorthy, M. A. Henderson, C. P. Berlinguette, *Inorg. Chem.* **2011**, 50, 3662–3672.
- [41] H.-W. Tseng, R. Zong, J. T. Muckerman, R. Thummel, *Inorg. Chem.* **2008**, 47, 11763–11773.
- [42] D. Hong, M. Murakami, Y. Yamada, S. Fukuzumi, *Energy Environ. Sci.* **2012**, 5, 5708–5716.
- [43] A. Ikeda-Ohno, S. Tsushima, C. Hennig, T. Yaitab, G. Bernhard, *Dalton Trans.* **2012**, 41, 7190–7192.
- [44] K. Kalyanasundaram, M. Grätzel, *Coord. Chem. Rev.* **1998**, 177, 347–414.
- [45] a) Z. Chen, J. J. Concepcion, J. W. Jurss, T. J. Meyer, *J. Am. Chem. Soc.* **2009**, 131, 15580–15581; b) A. K. M. Fung, B. K. W. Chiu, M. H. W. Lam, *Water Res.* **2003**, 37, 1939–1947.
- [46] Y. S. Nam, A. P. Magyar, D. Lee, J.-W. Kim, D. S. Yun, H. Park, T. S. Pollom, D. A. Weitz, A. M. Belcher, *Nat. Nanotechnol.* **2010**, 5, 340–344.
- [47] A. Juris, V. Balzani, F. Barigelli, S. Campagna, P. Belser, A. von Zelewsky, *Coord. Chem. Rev.* **1988**, 84, 85–277.
- [48] T. J. Meyer, *Pure Appl. Chem.* **1986**, 58, 1193–1206.
- [49] M. Marco, A. Cedi, L. Prodi, M. T. Gandolfi, *Handbook of Photochemistry*, 3rd ed., CRC Press, Taylor & Francis Group, Boca Raton, **2006**, pp. 379–404.
- [50] V. Balzani, A. Juris, *Coord. Chem. Rev.* **2001**, 211, 97–115.
- [51] G. C. Dismukes, R. Brimblecombe, G. A. N. Felton, R. S. Pryadun, J. E. Sheats, L. Spiccia, G. F. Swiegers, *Acc. Chem. Res.* **2009**, 42, 1935–1943.
- [52] M. Calvin, *Science* **1974**, 184, 375–381.
- [53] L. Duan, F. Bozoglian, S. Manda, B. Stewart, T. Privalov, A. Llobet, L. Sun, *Nat. Chem.* **2012**, 4, 418–423.
- [54] F. Liu, T. Cardolaccia, B. J. Hornstein, J. R. Schoonover, T. J. Meyer, *J. Am. Chem. Soc.* **2007**, 129, 2446–2447.
- [55] I. Ogino, K. Nagoshi, M. Yagi, M. Kaneko, *J. Chem. Soc. Faraday Trans.* **1996**, 92, 3431–3443.
- [56] T. Wada, K. Tsuge, K. Tanaka, *Angew. Chem.* **2000**, 112, 1539–1542; *Angew. Chem. Int. Ed.* **2000**, 39, 1479–1482.
- [57] T. Wada, K. Tsuge, K. Tanaka, *Inorg. Chem.* **2001**, 40, 329–337.
- [58] J. Mola, E. Mas-Marza, X. Sala, I. Romero, M. Rodríguez, C. Viñas, T. Parrella, A. Llobet, *Angew. Chem.* **2008**, 120, 5914–5916; *Angew. Chem. Int. Ed.* **2008**, 47, 5830–5832.
- [59] J. J. Concepcion, J. W. Jurss, P. G. Hoertz, T. J. Meyer, *Angew. Chem.* **2009**, 121, 9637–9640; *Angew. Chem. Int. Ed.* **2009**, 48, 9473–9476.
- [60] F. Li, B. Zhang, X. Li, Y. Jiang, L. Chen, Y. Li, L. Sun, *Angew. Chem.* **2011**, 123, 12484–12487; *Angew. Chem. Int. Ed.* **2011**, 50, 12276–12279.
- [61] J. D. Blakemore, N. D. Schley, G. W. Olack, C. D. Incavito, G. W. Brudvig, R. H. Crabtree, *Chem. Sci.* **2011**, 2, 94–98.
- [62] K. S. Joya, N. K. Subbaiyan, F. D'Souza, H. J. M. de Groot, *Angew. Chem.* **2012**, 124, 9739–9743; *Angew. Chem. Int. Ed.* **2012**, 51, 9601–9605.
- [63] S. M. Barnett, K. I. Goldberg, J. M. Mayer, *Nat. Chem.* **2012**, 4, 498–502.

- [64] a) D. G. Nocera, *Acc. Chem. Res.* **2012**, *45*, 767–776; b) H. J. M. de Groot, *Appl. Magn. Reson.* **2010**, *37*, 497–503.
- [65] B. Limburg, E. Bouwman, S. Bonnet, *Coord. Chem. Rev.* **2012**, *256*, 1451–1467.
- [66] L. Li, L. Duan, Y. Xu, M. Gorlov, A. Hagfeldt, L. Sun, *Chem. Commun.* **2010**, *46*, 7307–7309.
- [67] W. F. Rüttinger, G. C. Dismukes, *Chem. Rev.* **1997**, *97*, 1–24.
- [68] W. F. Ruettinger, C. Campana, G. C. Dismukes, *J. Am. Chem. Soc.* **1997**, *119*, 6670–6671.
- [69] a) R. Brimblecombe, G. F. Swiegers, G. C. Dismukes, L. Spiccia, *Angew. Chem.* **2008**, *120*, 7445–7448; *Angew. Chem. Int. Ed.* **2008**, *47*, 7335–7338; b) R. Brimblecombe, A. Koo, G. C. Dismukes, G. F. Swiegers, L. Spiccia, *J. Am. Chem. Soc.* **2010**, *132*, 2892–2894.
- [70] R. K. Hocking, R. Brimblecombe, L.-Y. Chang, A. Singh, M. H. Cheah, C. Glover, W. H. Casey, L. Spiccia, *Nat. Chem.* **2011**, *3*, 461–466.
- [71] N. S. McCool, D. M. Robinson, J. E. Sheats, G. C. Dismukes, *J. Am. Chem. Soc.* **2011**, *133*, 11446–11449.
- [72] R. Chakrabarty, S. J. Bora, B. K. Das, *Inorg. Chem.* **2007**, *46*, 9450–9462.
- [73] K. Dimitrou, K. Folting, W. E. Streib, G. Christou, *J. Am. Chem. Soc.* **1993**, *115*, 6432–6433.
- [74] A. R. Howells, A. Sankarraj, C. Shannon, *J. Am. Chem. Soc.* **2004**, *126*, 12258–12259.
- [75] A. Sartorel, M. Carraro, G. Scorrano, R. D. Zorzi, S. Geremia, N. D. McDaniell, S. Bernhard, M. Bonchio, *J. Am. Chem. Soc.* **2008**, *130*, 5006–5007.
- [76] Y. V. Geletii, B. Botar, P. Kögerler, D. A. Hillesheim, D. G. Musaev, C. L. Hill, *Angew. Chem.* **2008**, *120*, 3960–3963; *Angew. Chem. Int. Ed.* **2008**, *47*, 3896–3899.
- [77] F. M. Toma, *Nat. Chem.* **2010**, *2*, 826–831.
- [78] Q. Yin, J. M. Tan, C. Besson, Y. V. Geletii, D. G. Musaev, A. E. Kuznetsov, Z. Luo, K. I. Hardcastle, C. L. Hill, *Science* **2010**, *328*, 342–345.
- [79] J. J. Stracke, R. G. Finke, *J. Am. Chem. Soc.* **2011**, *133*, 14872–14875.
- [80] J. Rossmeis, K. Dimitrievski, P. Siegbahn, J. K. Nørskov, *J. Phys. Chem. C* **2007**, *111*, 18821–18823.
- [81] M. T. M. Koper, *J. Electroanal. Chem.* **2011**, *660*, 254–260.
- [82] J. Rossmeis, Z.-W. Qu, H. Zhu, G.-J. Kroes, J. K. Nørskov, *J. Electroanal. Chem.* **2007**, *607*, 83–89.
- [83] J. K. Nørskov, J. Rossmeis, A. Logadottir, L. Lindqvist, *J. Phys. Chem. B* **2004**, *108*, 17886–17892.
- [84] Á. Valdés, G.-J. Kroes, *J. Phys. Chem. C* **2010**, *114*, 1701–1708.
- [85] S. Piccinin, S. Fabris, *Phys. Chem. Chem. Phys.* **2011**, *13*, 7666–7674.
- [86] R. M. Dreizler, E. K. V. Gross, *Density Functional Theory*, Springer, Berlin, **1990**.
- [87] J. D. Blakemore, N. D. Schley, D. Balcells, J. F. Hull, G. W. Olack, C. D. Incarvito, O. Eisenstein, G. W. Brudvig, R. H. Crabtree, *J. Am. Chem. Soc.* **2010**, *132*, 16017–16029.
- [88] M. Z. Ertem, L. Gagliardi, C. J. Cramer, *Chem. Sci.* **2012**, *3*, 1293–1299.
- [89] D. Marx, J. Hutter, *Ab Initio Molecular Dynamics: Basic Theory and Advanced Methods*, Cambridge University Press, Cambridge, **2009**.
- [90] A. Laio, M. Parrinello, *Proc. Natl. Acad. Sci. USA* **2002**, *99*, 12562–12566.
- [91] A. Barducci, G. Bussi, M. Parrinello, *Phys. Rev. Lett.* **2008**, *100*, 1–4.
- [92] P. Raiteri, A. Laio, F. L. Gervasio, C. Micheletti, M. Parrinello, *J. Phys. Chem. B* **2006**, *110*, 3533–3539.
- [93] S. Piana, A. Laio, *J. Phys. Chem. B* **2007**, *111*, 4553–4559.
- [94] S. Singh, C. Chiu, J. J. de Pablo, *J. Stat. Phys.* **2011**, *145*, 932–945.
- [95] J. L. Vallés-Pardo, M. C. Guijt, M. Iannuzzi, K. S. Joya, H. J. M. de Groot, F. Buda, *ChemPhysChem* **2012**, *13*, 140–146.
- [96] X. Biarnés, A. Ardèvol, J. Iglesias-Fernández, A. Planas, C. Rovira, *J. Am. Chem. Soc.* **2011**, *133*, 20301–20309.
- [97] P. Söderhjelm, G. A. Tribello, M. Parrinello, *Proc. Natl. Acad. Sci. USA* **2012**, *109*, 5170–5175.
- [98] R. Edberg, D. J. Evans, G. P. Morriss, *J. Chem. Phys.* **1986**, *84*, 6933–6939.
- [99] M. Sprik, G. Ciccotti, *J. Chem. Phys.* **1998**, *109*, 7737–7744.
- [100] W. K. den Otter, W. J. Briels, *J. Chem. Phys.* **1998**, *109*, 4139–4146.
- [101] a) D. S. Ginley, D. Cahen, *Fundamentals of Materials for Energy and Environmental Sustainability*, Cambridge University Press, Cambridge, **2011**; b) K. S. Joya, PhD thesis, Leiden University (The Netherlands), **2011**.
- [102] D. Noy, C. C. Moser, P. L. Dutton, *Biochim. Biophys. Acta Bioenerg. Biochim. Biophys. Acta* **2006**, *1757*, 90–105.
- [103] T. J. Eisenmayer, H. J. M. de Groot, E. van de Wetering, J. Neugebauer, F. Buda, *J. Phys. Chem. Lett.* **2012**, *3*, 694–697.
- [104] C. C. Moser, J. M. Keske, K. Warncke, R. S. Farid, P. L. Dutton, *Nature* **1992**, *355*, 796–802.
- [105] M. Katterle, V. Prokhorenko, A. Holzwarth, A. Jesorka, *Chem. Phys. Lett.* **2007**, *447*, 284–288.
- [106] S. V. Bhosale, C. H. Janiab, S. J. Langford, *Chem. Soc. Rev.* **2008**, *37*, 331–342.
- [107] N. Sakai, J. Mareda, E. Vauthey, S. Matile, *Chem. Commun.* **2010**, *46*, 4225–4237.
- [108] S. L. Suraru, U. Zschieschang, H. Klauk, F. Wurthner, *Chem. Commun.* **2011**, *47*, 11504–11506.
- [109] M. A. Rodrigues, D. F. S. Petri, M. J. Politi, S. Brochsztain, *Thin Solid Films* **2000**, *371*, 109–113.
- [110] S. Brochsztain, M. A. Rodrigues, G. J. F. Demets, M. J. Politi, *J. Mater. Chem.* **2002**, *12*, 1250–1255.
- [111] T. D. M. Bell, S. Yap, C. H. Jani, S. V. Bhosale, J. Hofkens, F. C. D. Schryver, S. J. Langford, K. P. Ghiggino, *Chem. Asian J.* **2009**, *4*, 1542–1550.
- [112] R. Scott Lokey, B. L. Iverson, *Nature* **1995**, *375*, 303–305.

Received: June 21, 2012

Revised: November 11, 2012

Published online on December 13, 2012